

Structure, Dynamics and Solvation of HIV-1 Protease/Saquinavir Complex in Aqueous Solution and Their Contributions to Drug Resistance: Molecular Dynamic Simulations

Kitiyaporn Wittayanarakul,[‡] Ornjira Aruksakunwong,[‡] Pornthep Sompornpisut,[‡]
Vannajan Sanghiran-Lee,[§] Vudhichai Parasuk,[‡] Surapong Pinitglang,[†] and Supot Hannongbua^{*,‡}

Department of Chemistry, Faculty of Science, Chulalongkorn University,
Pratumwan, Bangkok 10330, Thailand, Department of Chemistry, Faculty of Science, Chiangmai University,
Chiang Mai 50200, Thailand, and Department of Food Technology, Faculty of Science,
The University of the Thai Chamber of Commerce, Dindang, Bangkok 10400, Thailand

Received July 11, 2004

As it is known that the understanding of the basic properties of the enzyme/inhibitor complex leads directly to enhancing the capability in drug designing and drug discovery. Molecular dynamics simulations have been performed to examine detailed information on the structure and dynamical properties of the HIV-1 PR complexed with saquinavir in the three protonated states, monoprotonates at Asp25 (Mono-25) and Asp25' (Mono-25') and diprotonate (Di-Pro) at both Asp25 and Asp25'. The obtained results support clinical data which reveal that Ile84 and Gly48 are two of the most frequent residues where mutation toward a protease inhibitor takes place. In contrast to the Ile84 mutation due to high displacement of Ile84 in the presence of saquinavir, source of the Gly48 mutation was observed to be due to the limited space in the HIV-1 PR pocket. The Gly48 was, on one side, found to form strong hydrogen bonds with saquinavir, while on the other side this residue was repelled by the hydrophobic Phe53 residue. In terms of inhibitor/enzyme binding, interactions between saquinavir and a catalytic triad of the HIV-1 PR were calculated using the *ab initio* method. The results show an order of the binding energy of Mono25 < Di-pro < Mono-25', suggesting that the active site in the HIV-1 PR complexed with saquinavir is monoprotonated states on Asp25. In contrast to the binding energy, 3, 6 and 12 hydrogen bonds between saquinavir and HIV-1 PR were found for the Mono-25, Mono-25' and Di-pro states, respectively. Discrepancy between the two trends suggests us to conclude that interaction between inhibitor and catalytic residues should be used as a criteria to enhance capability in drug designing and drug screening instead of using the total inhibitor/enzyme interaction which is normally reported in the literature. In addition, the distribution and binding of water molecules, in terms of hydrogen bonding, to the donor atoms of saquinavir were investigated and discussed, referring to that which was reported experimentally.

INTRODUCTION

The protease of human immunodeficiency virus 1 (HIV-1) plays an essential role in maturing infectious HIV particles.¹ Its structure and function have been well characterized, classified into subsite (P1, P1', P2, P2', P3, see Figure 1) and widely used to develop potent inhibitors as the therapeutic agent for AIDS.² The HIV-1 protease belongs to the class of aspartic proteases which contains a pair of catalytic Asp residues. In the active homodimeric HIV-1 protease (HIV-1 PR),³ the catalytic aspartyl dyad (Asp25 and Asp25') is located at the subunit-subunit interfacial region which is at the base of the substrate binding site. The active site is within a largely hydrophobic cavity capped by two flexible flaps (Figure 1). The specific task of the flaps is guarding the entrance to the active site cleft. The development of new and powerful HIV-1 PR inhibitors is relied strongly on the enzyme/inhibitor interactions. Therefore, the understanding of basic properties such as structure, dynamics and solvation of the complex helps directly in drug designing

and drug discovery. To obtain the above-mentioned information experimentally, especially in solution, it is rather complicated. Therefore, theoretical methods such as molecular dynamics simulations proved to be a powerful tool for such propose.

Difficulty takes place in dealing with HIV-1 PR in which protonation equilibria in the active site depends on the three possible protonated states of the dyad residues, monoprotonated at each Asp25 or Asp25' and diprotonate. The knowledge of the ionization state of the two catalytic aspartates is extremely important for drug design in a way to optimize the interactions between the inhibitor and the enzyme. Considerable efforts have been spent on this problem.^{4–7} These studies reported different protonation models depending upon the local environment of the enzyme–inhibitor complex.⁸ Ky-Youb Nam et al.⁹ performed *ab initio* calculations and the free energy perturbation to determine the protonated state of HIV-1 protease complexed with inhibitor, A74704. The results show the significant implication that the protonated state of the active site of the complex is monoprotonated on Asp25. Plane wave-based *ab initio* molecular dynamics calculations¹⁰ as well as NMR measurements¹¹ of the active site region of the HIV-1 PR

* Corresponding author e-mail: supot@atc.atccu.chula.ac.th.

[†] The University of the Thai Chamber of Commerce.

[‡] Chulalongkorn University.

[§] Chiangmai University.

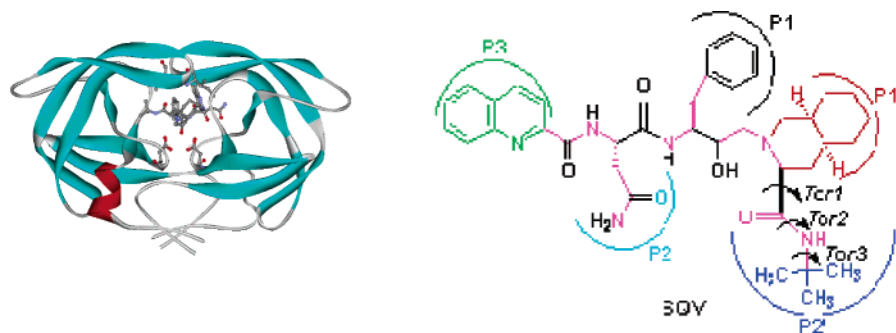


Figure 1. HIV-1 protease complexed with saquinavir, classification of P1, P1', P2, P2' and P3 subsites and definition of torsional angles (*Tor1-Tor3*), where catalytic dyad, Asp25 and Asp25', are displayed as ball-and-stick and the two Ile50 and Ile50' at the flap regions were also labeled.

complexed with pepstatin suggest that the system is at least monoprotonated, i.e., one of the two catalytic oxygens on an Asp residue is protonated.

This paper aims to investigate the structure, dynamics and solvation of HIV-1 PR complexed with saquinavir (Figure 1), the first HIV-1 PR inhibitor licensed for clinical use.¹² The contribution of such properties to drug resistance was also taken into consideration. The simulations were performed for the three protonated states. The unprotonated one was excluded due to the literature.^{9–11}

METHODS

The Initial Structure. The structure of HIV-1 protease complexed with saquinavir (SQV) was taken from the Brookhaven Protein Data Bank (PDB code: 1HXB). The preparation of the initial structure starts by adding hydrogen atoms to the complex using AMBER 7.0 program.¹³ The RESP charges were applied to all atoms of the HIV-1 protease, while the atomic charges of atoms of saquinavir, which are not available in the program, were prepared by fitting the electrostatic potentials around the molecule to the standard model using the RESP method.¹⁴ The electrostatic potential was obtained by the Hartree–Fock single point calculation with 6-31G(d,p) basis set using Gaussian 98 program.¹⁵

Molecular Dynamic Simulations. Three simulations have been performed for the three protonated states of binding of HIV-1 PR/saquinavir complexes: monoprotonates at Asp25 (Mono-25) and 25' (Mono-25') and diprotonate at both Asp25 and Asp25' (Di-Pro). To examine detailed information on the changes of the structure and dynamical properties of the HIV-1 PR via complexation, additional simulation was performed for the HIV-1 PR in its free form in the Mono-25 state. The simulated systems were neutralized by 7 Na⁺ and additional 11 Cl⁻ and 12 Cl⁻ for mono- and diprotonation, respectively. All models were solvated by TIP3P water molecules in the 74.52 Å × 77.38 Å × 66.26 Å box. Prior to MD simulations, each system was energy minimized. The total atoms of these simulations are 32946 and 32945 for mono- and diprotonation, respectively. The MD simulations were carried out for 1 ns. All simulations and energy minimization were performed using the AMBER 7.0 program¹³ with all atomic force field developed by Cornell et al.¹⁶ The simulations were performed with a time step of 2 fs and with a cutoff radius of 12 Å for the nonbonded interactions. The temperature was maintained at 298 K. The Particle Mesh Ewald (PME) method was employed for

correcting electrostatic interaction. Periodic boundary conditions were applied, and the pressure was maintained at 1 atm by adjustment of the volume of the periodic box.¹⁷

Quantum Chemical Calculations. To investigate precise interaction energy in the different protonated states, the complexes were represented by 2 triads, Asp25-Thr26-Gly27 of both chains and saquinavir. The selected residues were obtained from the MD simulation using the following steps: (i) calculate the average structure from the whole trajectory, (ii) perform geometry optimization using energy minimization from AMBER 7.0 program, (iii) remove coordinates of the nonselected residues, keep only those of the 6 residues at the active site triad of the two chains and the saquinavir, (iv) terminate the C- and the N-termini at the ends of the selected residues by CH₃NH- and -COCH₃ groups, and (v) optimize geometry of the newly added hydrogen atoms using ab initio calculations at the second-order Møller–Plesset perturbation level with 6–31 G(d,p) basis set. Then, interaction between the selected residues and saquinavir for the three simulated systems were calculated using the density functional theory B3LYP/6-31G(d,p) with the extended 6-31+G-(d,p) basis sets. Calculations were performed using the Gaussian 98 program.¹⁵

RESULTS AND DISCUSSION

Flexibility of Saquinavir in the Complex. To explore flexibility of saquinavir's subsites (defined in Figure 1) in the complex, root-mean-square displacement (RMSD) of each subsite, relative to the initial MD (X-ray) structure, was calculated and shown in Figure 2. The RMSD plots through the simulation time, after equilibration, indicate very clearly that conformations of all subsites in the three protonated states are almost unchanged, except that of P2'.

Detailed discussion is centered on the conformational changes of P2' subsite in which that of each protonated state exhibits different characters. Significant and permanent changes were observed for the Mono-25 state where the RMSD of approximately 1.1 Å starts to be detected through the whole range of the simulation, after equilibration (Figure 2a).

This fact indicates the single preferential conformation of the P2' subsite of saquinavir in the complex with HIV-1 PR in the Mono-25 state. Situations are different for the Mono-25' and Di-pro states where fluctuations of the RMSD were obviously detected. Figure 2b suggests two preferential conformations of the P2' subsite of saquinavir in the

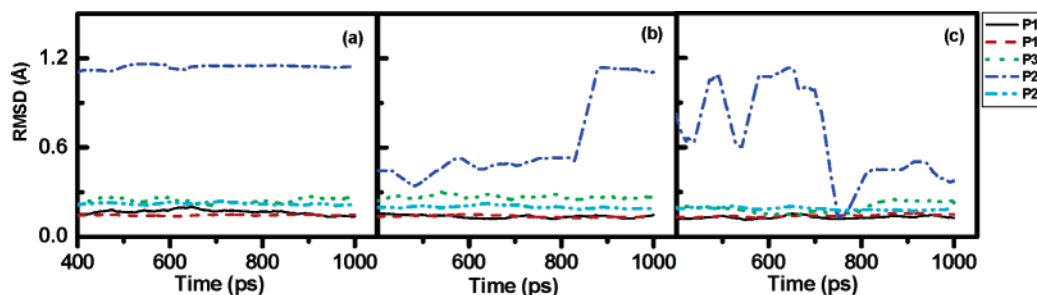


Figure 2. RMSD for the three protonated states, Mono-25 (a), Mono-25' (b) and Di-pro (c), of saquinavir's subsites (defined in Figure 1) relative to the initial MD (X-ray) structure.

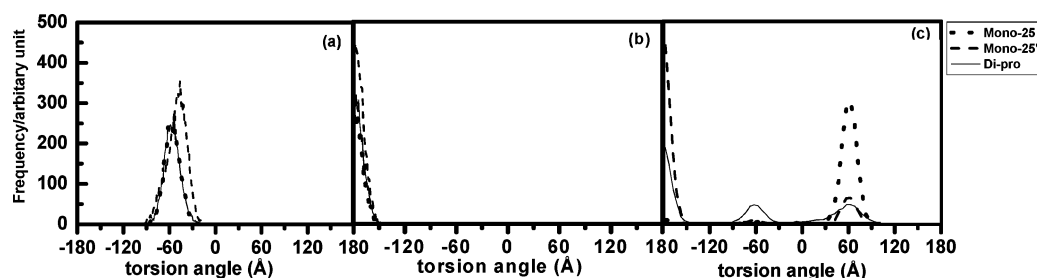


Figure 3. Changes of P2' torsional angles, *Tor1-Tor3* (a-c) defined in Figure 1, of saquinavir complexed with HIV-1 PR.

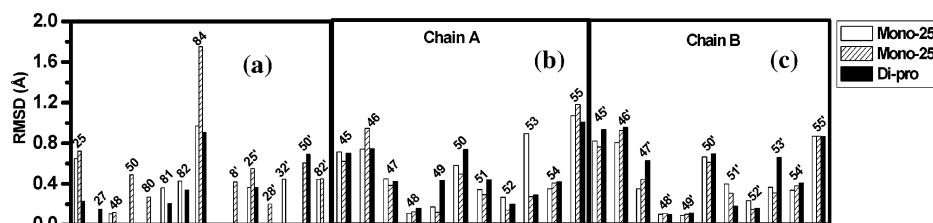


Figure 4. Comparison of RMSD for the Mono-25, Mono-25' and Di-pro states with respect to their average structure for the residues located within 3 Å around saquinavir (a) and in the flap region, residues 45–55 (b).

monoprotonated state on Asp25' of HIV-1 PR with the RMSDs of approximately 0.5 and 1.1 Å. Furthermore, the Di-pro state favors two major conformations at the RMSDs of about 0.4 and 1.1 Å and two additional minor probabilities at RMSDs of about 0.6 and 0.1 Å (Figure 2c).

To look into a detailed source of the above findings, changes of P2' torsional angles, *Tor1-Tor3* defined in Figure 1, of saquinavir were analyzed and displayed in Figure 3. The plots show pronounced and sharp peaks indicating rigidity of the three angles, i.e., they are slightly flexible in a narrow range. No significant difference of the *Tor1* and *Tor2* angles was found for the three protonated states of the HIV-1 PR (Figures 3a-3b). For the angle *Tor3* (Figure 3c), the changes are consistent with the RMSD plots for P2' at the three states shown in Figure 2 leading to the following conclusions. Single preferential conformation of P2' subsite for the Mono-25 states (Figure 2a) was represented by the single sharp peak at *Tor3* = 60° (dot line, Figure 3c). Furthermore, the two peaks at *Tor3* = -180° and 60° (broken line) in Figure 3c are due to the two conformations of the Mono-25' state where RMSDs = 0.5 and 1.1 Å (Figure 2b), respectively. A sharper and higher peak at *Tor3* = -180° than the other one at *Tor3* = 60° indicate higher rigidity and higher probability of finding of the first conformation (RMSD = 0.5 Å from 400 to 840 ps in Figure 2b) than the other one (RMSD = 1.1 Å from 900 ps to 1000 ps in Figure 2b), respectively. In addition, the three peaks at *Tor3* = -180°, -60° and 60° of the Di-pro state (solid line in Figure 3c) can be assigned to the RMSDs = 0.4, 1.1,

and 0.6 Å for the Di-pro state taken place in Figure 2c, respectively.

Flexibility of HIV-1 PR in the Complex. Protein flexibility is known to play a role not only in the catalytic process but also in the computer-aided drug design. A clear example is the high flexibility of the flaps (residues 45–55) in both monomeric and dimeric forms of unliganded protease reported by both computational^{18,19} and experimental^{20,21} studies. We now turn our attention to investigate their property quantitatively. Attention is focused on the flexibility of the residues lying in the flap region and those located within 3 Å from all atoms of saquinavir. The RMSD for those residues with respect to the X-ray structure for three states were evaluated and plotted in Figure 4a-4b.

It is interesting to note that within a spherical radius of 3 Å from the saquinavir highest and lowest displacements were observed at Ile84 and Gly48 residues of chain A (Figure 4a-4b), respectively (Gly48 is not within 3 Å limit for Di-Pro state). Surprisingly, these observations support clinical data which reveal that Ile84 and Gly48 are two of the most frequent residues where mutation toward a protease inhibitor²² takes place. The data lead us to conclude that a conformational change is a primary source of mutation of Ile84. In contrast, Gly48 mutation can be described in terms of indirect displacement of Phe53 in the flap region. As can be seen in Figure 4b that the RMSDs of Phe53 of the Mono-25 chain A and of Di-pro chain B are significantly higher than those of the other two states. A clear description of the mutation of Gly48 was given in the next paragraph.

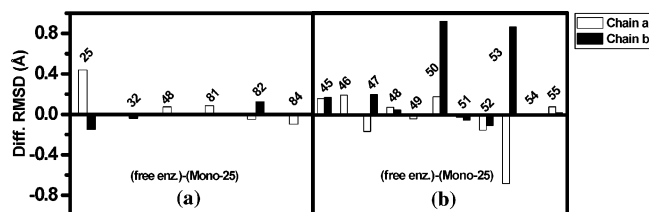


Figure 5. Subtraction between the RMSDs of the free enzyme and complex for the Mono-25 state lying within 3 Å from the atoms of saquinavir (a) and the flap region, residues 45–55 (b).

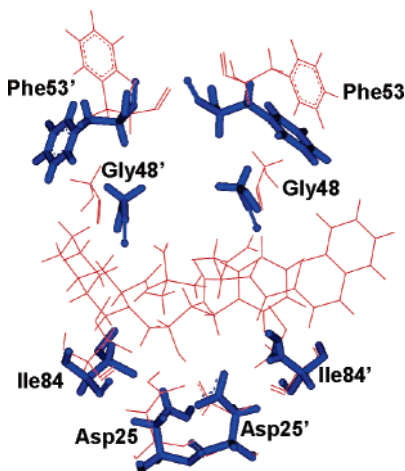


Figure 6. Superimposition between the average structures of HIV-1 PR in free (stick) and complex forms (line) where only selected residues are displayed.

To explore the conformational changes due to complexation, subtraction between the RMSDs for the residues of the free enzyme and the complex of the Mono-25, lying in the flap region and those located within 3 Å from the atoms of saquinavir were again calculated and plotted in Figure 5a–5b, i.e., a positive value indicates higher rigidity of the complex than the free enzyme. Dramatic changes were detected on the residues Ile50', Phe53' (Figure 5b) and Asp25

(Figure 5a) where the RMSD of free enzyme are much higher than those of the complex. This observation can be easily explained in terms of binding between enzyme and inhibitor which leads directly to rigidity of the complex. Surprisingly, residue Phe53 (Figure 5b) in the flap region in the complex form is less rigid than the free form. This is in contrast to what is generally known and reported by Zhongwei Zhu et al.²³ using free energy techniques showing that a barrier to flap opening exists in the presence of an inhibitor while this evidence disappears for the free enzyme. This observation confirms the lower rigidity of Phe53 chain A of Mono-25 state in the complex than the free forms (Figure 5b). To understand the reason for the mutation due to the indirect displacement, superimposition between the enzyme structures in the free and complex forms was examined, and the molecular structure in an area close to Phe53 of both chains was displayed in Figure 6. It can be clearly seen from the plot that the presence of saquinavir leads to dramatic changes of the conformations of Phe53 and Phe53'.

Gly48, on one side, was found to form strong hydrogen bonds with saquinavir (details in HIV-1 PR Binding section), while it was, on the other side, repelled by the hydrophobic Phe53 residue. This leads directly to a very high rigidity of Gly48 (Figure 4b, chain A) as well as a high displacement of Phe53. Such unfavorable conditions were supposed to facilitate the mutation of Gly48. Due to the unsymmetric character of the saquinavir molecule, Gly48' was not detected to bind to the other end of saquinavir. Therefore, Gly48' is less interfered by the presence of saquinavir in comparison to Gly48. This can be also a reason for the lower RMSD of Phe53' than Phe53 (Figure 4b, Mono-25) and the higher degree of drug resistance of Gly48 than Gly48'. This evidence is fully supported by the X-ray crystallographic analysis and molecular modeling experiments.²² A clear conclusion is that in addition to the I84V mutation due to high displacement of Ile84 in the presence of saquinavir (Figure 4a), cooperation effect can be also due to the limited

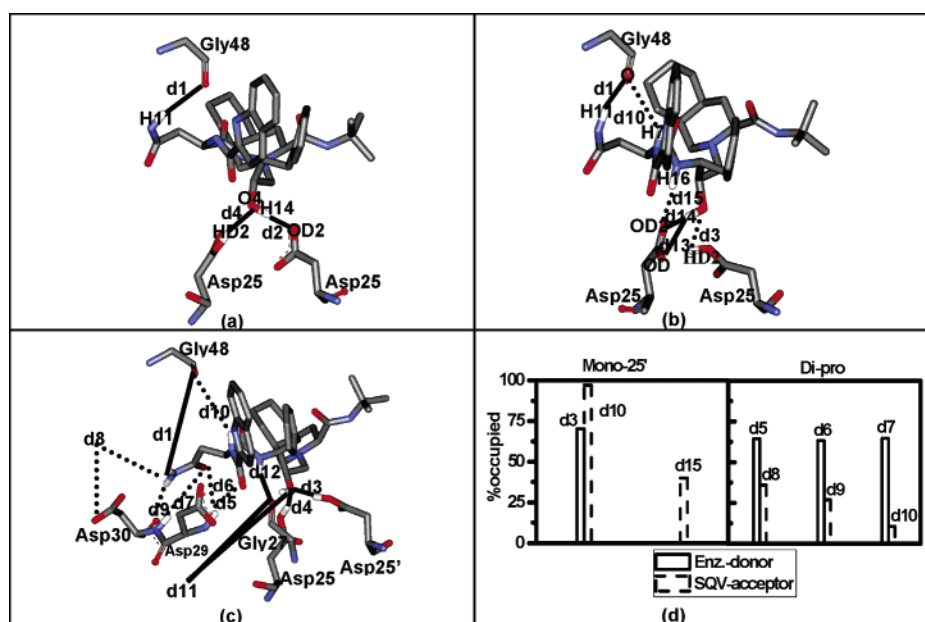


Figure 7. Binding between saquinavir and HIV-1 PR in the Mono-25 (a), Mono-25' (b) and Di-pro (c) states where solid and broken lines denote hydrogen bonds which were detected 100% and less than 100% of the total configurations (400–1000 ps) after equilibration, respectively. Percentages of occupation were given in a bar graph (d) where roles of saquinavir (SQV) and HIV-1 PR (ENZ) as proton donor/acceptor were separately plotted.

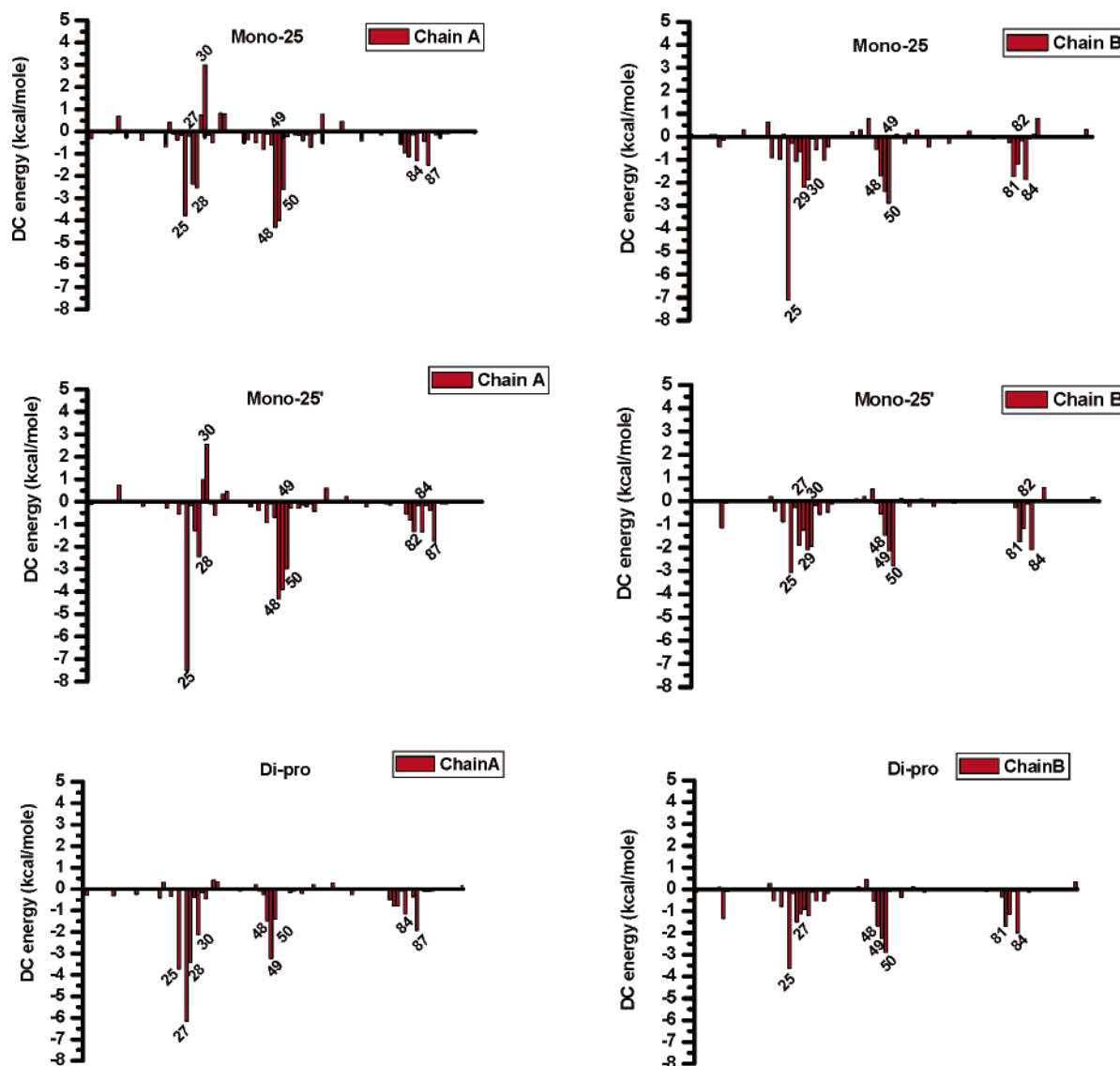


Figure 8. The summations of the van der waal and electrostatic terms are plotted between all residues of HIV-1 PR and SQV.

space (Figure 6) in the HIV-1 PR pocket, especially for the G48V where saquinavir requires more space on the Gly48 than the Gly48' sides.

Saquinavir-HIV-1 PR Binding. Most enzymes are highly specific for their substrate; therefore, an inhibitor of a similar shape and chemical nature is usually supposed to be recognized by the enzyme. This approach was widely used to design inhibitors for diverse enzymatic targets, including HIV-1 protease. To further explore the binding between saquinavir and HIV-1 PR, hydrogen bonds of the three protonated states were analyzed based on the donor–acceptor distance criteria. The results were illustrated in Figure 7a–7c. Percentages of occupation in which saquinavir and HIV-1 PR play a role as proton donor/acceptor were separately given in Figure 7d. The plots (Figure 7a–7c) show 3, 6 and 12 hydrogen bonds between saquinavir and HIV-1 PR in the Mono-25, Mono-25' and Di-pro states, where 3, 3 and 6 of them are 100% occupied, respectively. Detailed comparison is concentrated on the different binding between saquinavir and HIV-1 PR in the two monoprotonated states, Mono-25 and Mono-25'. In the first system, saquinavir was held in the cavity of the HIV-1 PR by the three hydrogen bonds with 100% occupation, via Gly48 and the two catalytic

residues, Asp25 and Asp25' (Figure 7). The other three bonds were additionally detected for the Mono-25' state. In this case, Gly48 forms one more pronounced hydrogen bond with H7 (95% occupation), while Asp25 forms one more pronounced bond with H14 (100% occupation) and another weak bond with H14 (30% occupation). Note that binding between Asp25' and the OH group of saquinavir in the Mono-25' state is slightly weaker (70% occupation) than that in the Mono-25 state. For the diprotonated state, saquinavir forms several hydrogen bonds with not only Gly48, Asp25 and Asp25' as in the monoprotonated one but also to Gly27, Asp29 and Asp30. The corresponding percentages of fully and partial occupations were shown in Figure 7c and 7d.

To seek for the fundamental basis of protein–drug interactions, the interaction energy between individual protease residue and saquinavir were calculated using the decomposition energy module of Amber 7 and, then, plotted as shown in Figure 8. The decomposition of the energy shows that the *per residue* interaction energy varies in the range 3 to –8 kcal/mol for all three protonation states. These plots suggested that the relatively significant interaction between the enzyme and SQV was due to the residues in the 3 regions of both chains, those in the catalytic site, the flaps and the

Table 1. Interaction between Saquinavir and the Catalytic Triad Residues, Asp25-Thr26-Gly27 of Both Chains of HIV-1 PR at the Three Protonated States Yielded from QM and MM Calculations^a

protonated state	QM (kcal/mol)	MM (kcal/mol)	MM/QM × 100 (%)
Mono-25	-66.9	-34.84	52
Mono-25'	-49.7	-28.09	56
Di-pro	-59.3	-25.11	42

^a For the QM, the density functional theory B3LYP/6-31G(d,p) with the extended 6-31+G(d,p) basis sets were applied (see text for more details).

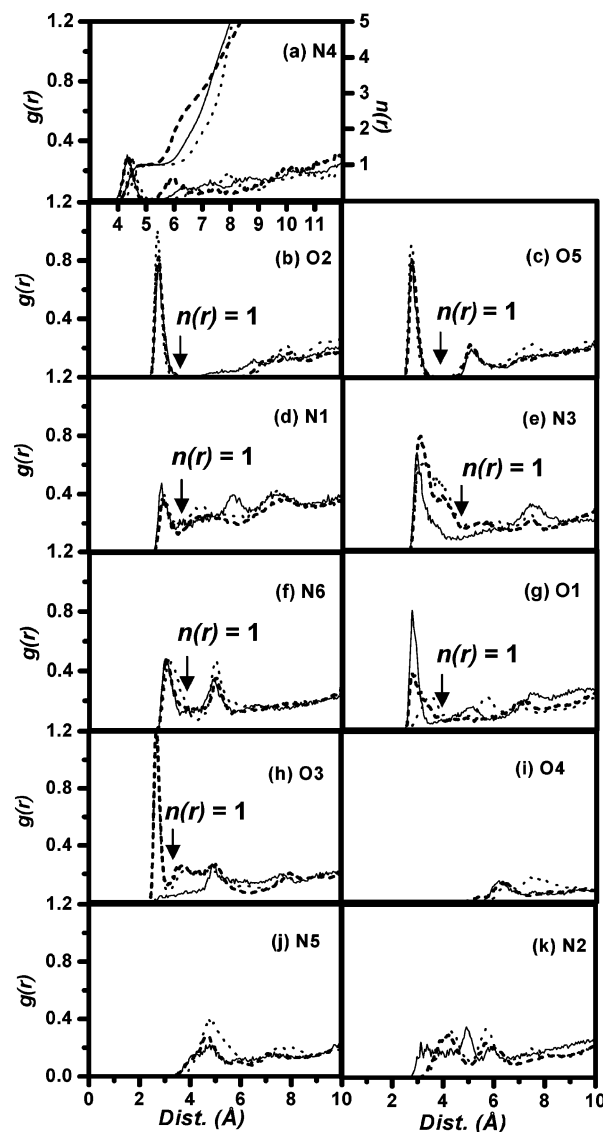
C-terminus (Pro81-Ile84). The fact that these three regions are recognized as the binding sites for SQV.

As discussed above, the significant conformational changes are associated with the mutation of Gly48 and Ile84. The decomposition of the SQV-enzyme interaction energy in Figure 8 provides a strong support in terms of energy contributions from those two residues. With an exception of the catalytic residues, which must be highly conserved in the aspartyl protease family, the mutation of Gly48 and Ile84 in the HIV-1 protease is, therefore, an optimal choice for the virus to achieve drug resistance.

To separate interaction between saquinavir and the catalytic site of the enzyme from the total enzyme/saquinavir interaction, *ab initio* calculations were performed (more details in the Quantum Chemical Calculations section). Table 1 shows the interaction energy between saquinavir and the catalytic triad residues, Asp25-Thr26-Gly27 of both chains, of HIV-1 PR. An unexpected result is an order of stability in which the interaction energy of -66.9 kcal/mol for Mono-25 is significantly deeper than that of -59.3 kcal/mol and -49.7 kcal/mol for the Di-pro and Mono-25', respectively, i.e., Mono-25 < Di-pro < Mono-25'.

In addition to the QM interaction energy, the energy derived from the force field implemented in the Amber program was also computed to estimate the MM potential quality (Table 1). The MM interaction energy was obtained by adding up the decomposed energy data (Figure 8) of the catalytic triad residues, in which the model is analogously used in the QM calculation. The results in Table 1 show that the MM interaction energies for the three states are approximately 50% lower than those yielded from the QM approach. In addition, the MM results suggest an order of the stability of Mono-25 < Mono-25' < Di-pro. This is different from that predicted from the QM calculation where Mono-25 < Di-pro < Mono-25'. Nevertheless, both approaches suggest the Mono-25 is the most energetically favorable configuration where the predicted energies are significantly lower than the other two states. It should be noted that the MM potential energy surface is usually generalized to be applicable for a wide range of molecular systems, leading to a lack of some specific details, especially for the present study where hydrogen bonding and ion-molecule interactions are known to play a role. These effects can be quantum mechanically taken into account.

Consequently, the trend suggested by the QM results is in contrast to an order of a number of hydrogen bonds between saquinavir and HIV-1 PR in which Di-pro > Mono-25' > Mono-25 (Figure 7). This can be due to structural changes of both saquinavir and catalytic residues via complexation in order to allow a better conformational fit

**Figure 9.** Radial distribution function, $g(r)$, and corresponding integration numbers (right axis for Figure 8a and marked by number and arrow for the other) from acceptor atoms of saquinavir (labeled as an inset and in Figure 9) to oxygen atom of water molecule for the three protonated states, Mono-25 (dot line), Mono-25' (short dash line) and Di-pro (solid line).

between saquinavir and HIV-1 PR in the catalytic than the other regions. The above finding has potentially significant implications that the protonated state of the active site in HIV-1 PR complexed with saquinavir inhibitor is a mono-protonated state on Asp25. However, since the protease has C_{2v} symmetry, the proton-transfer mechanism is much faster than reorientation of the inhibitor at the active site.²⁴ Therefore, the proton transfer is associated with the Asp25/Asp25' conversion. In addition, interaction between the inhibitor and the catalytic region of the enzyme is supposed to relate directly to the activity of the inhibitor in the catalytic process. Therefore, interaction between the inhibitor and the catalytic residues should be used as a criteria to enhance capability in drug designing and drug screening instead of using the total inhibitor/enzyme interaction which is normally reported in the literatures.

Some comments should be made concerning contributions of the environment to the free energy of binding as well as the QM interaction energy shown in Table 1. These effects

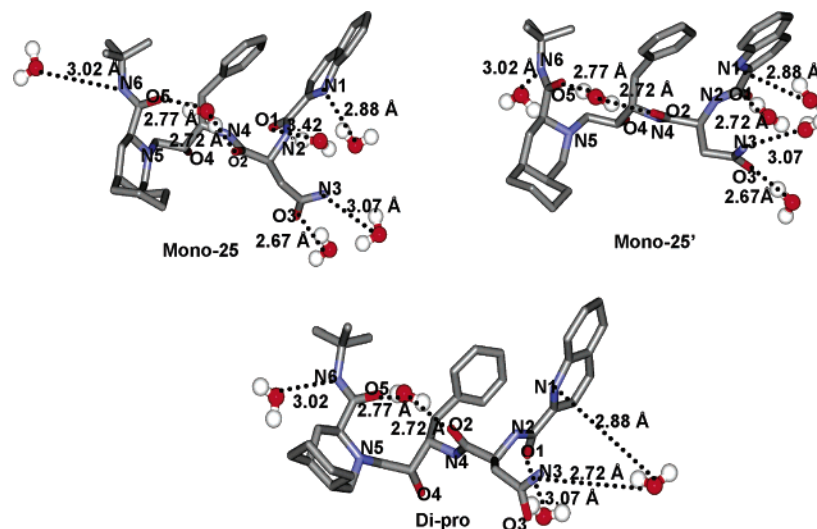


Figure 10. Snapshot which accumulates water molecules lying in the first hydration shell of saquinavir inhibitor in the three protonated states.

were taken into account in our previous work²⁵ using ONIOM and MM/PBSA methods embedded in the Gaussian 98 the AMBER programs, respectively.

Characteristic of Water Molecules in the Cavity of HIV-1 PR. An important question that arises in the context of drug binding studies involves the distribution of water molecules in the cavity region. To seek for such information the plot of radial distribution function (RDF, $g_{xy}(r)$)—the probability of finding a particle of type x in a spherical radii, r , around the particle of type y —from acceptor atoms of saquinavir (see labels in Figure 10) to an oxygen atom of water was used. The results, for the three protonated states were calculated, were shown in Figure 9 together with the corresponding running integration numbers.

Investigation was primarily focused on N4 of saquinavir since it was, topologically, located almost at the center of the binding pocket of the HIV-1 PR (see labels in Figure 9). The plots for the three states (Figure 9a) show the first sharp peak centered at 4.3 Å with the running coordination number of 1 water molecule, integrated up to the first minimum of 4.8 Å. Although the peak is very sharp and well pronounced but with the distance of 4.3 Å, it can be concluded very clearly that no water molecule is bound directly to the N4 atom. The plots of the coordination number (right scale of Figure 9a) start to increase exponentially between 6 and 7 Å indicating the boundary between the water inside the cavity and bulk water. This distance is consistent with half of the estimated diameter (from the tips of the flap to the active site residues) of the HIV-1 PR pocket of 13.5 Å.²³ To estimate the total number of water molecules in the pocket of the HIV-1 PR, an oxygen atom of a water molecule lying within the spherical radius of 3.0 Å (distance to the first minimum of the RDFs from donor atoms of saquinavir to oxygen atoms of saquinavir to oxygen atom of water as shown in Figure 9 around the atoms of saquinavir were counted and averaged using the water-shell option in the Amber program). The Mono-25, Mono-25' and Di-pro pockets were found to contain 17, 15 and 15 water molecules, respectively.

The RDF plots in Figure 9b-9k can be classified into 3 types, i.e., the RDFs exhibit (i) the first sharp peak at ~ 3 Å where the minimum approaches zero (Figure 9b-9c); (ii) the

first sharp peak at ~ 3 Å where the minimum is above zero (Figure 9d-9h exclude Di-pro of O3) and (iii) the first broad peak either at ~ 3 Å or > 3 Å (Figure 9i-9k). The first type RDF with the corresponding coordination number of one indicates that O2 and O5 of saquinavir are solvated by one water molecule in terms of hydrogen bonding (O—O distance = 3.0 Å) with 100% occupation (the first minimum approaches zero). For the second type RDF, the coordination number of one indicates a single hydrogen bond, almost 100% occupation, between a saquinavir and a water molecule, while the nonzero minimum demonstrates solvent exchange, hydrogen bond breaking and forming, between the first and the second peaks (second solvation shells). In contrast, O4, N5 and N2 were observed to be free form solvation, third type RDF (Figure 9i-9k). To visualize the above-mentioned hydration, a snapshot which accumulates water molecules lying under the first peak at 3 Å of the RDFs was displayed in Figure 10.

Comprehensive investigation has been made to seek for the precise orientation of the one water molecule in the nearest of O2 and O5. It is interesting to note that O2 and O5 were observed to solvate by the same water molecule in the configuration shown in Figure 9. This water molecule was, at the same time, found to form a hydrogen bond with the flap residues, Ile50 and Ile50' (see Figure 1). This is in good agreement with the experimental observation where these unique water molecules are commonly detected to hold the molecular structure in the peptidomimetic inhibitor complexes.²⁶ Interest is also focused on the solvation of O4 which is the OH group of saquinavir known to bind to the catalytic dyad residues of the HIV-1 PR and to take part in inhibiting the catalytic process.²³ Within a spherical radius of 5 Å around O4, no water molecule was detected (Figure 9h).

This fact supports the previous finding which states that inhibition of the catalytic mechanism of the protease is most likely a combination of favorable binding of a particular compound and exclusion of water from the active site.²³ In contrast, a single water molecule, known as catalytic water,²⁷ is required in the catalytic mechanism of the HIV-1 PR. However the HIV-1 PR mechanism was also proposed to involve the nucleophilic attack.²⁸

CONCLUSIONS

MD simulations of the HIV-1 PR complexed with saquinavir in the three protonated states, monoprotonates at Asp25 and Asp25' and diprotonate at both Asp25 and Asp25', provide information on structural and dynamical characteristics in term of flexibility, saquinavir/HIV-1 PR binding and hydration structure of the complexes. The simulation results report good evidence that deal with questions related to the basic mutation and solvation data. With reference to the molecular structure of the HIV-1 PR in free form, the presence of saquinavir leads to dramatic changes of the conformations of Phe53 and Phe53'. In terms of the flexibility of saquinavir in the complexes, significant changes of the conformation of P2' subsite were obviously detected. For the enzyme, the highest and lowest displacements were observed at Ile84 and Gly48 residues of chain A, respectively. These observations support clinical data which reveal that Ile84 and Gly48 are two of the most frequent residues where mutation toward a protease inhibitor takes place. The detected data suggest us to conclude that conformational change is a primary source of mutation of Ile84. In contrast, Gly48 mutation can be described in terms of indirect displacement of Phe53 in the flap region. Furthermore, 3, 6 and 12 hydrogen bonds between saquinavir and the HIV-1 PR were observed in the Mono-25, Mono-25' and Dipro states, where 3, 3 and 6 of them are 100% occupied, respectively. To separate interaction between saquinavir and the catalytic site of enzyme from the total enzyme/saquinavir interaction, ab initio calculations were performed. An unexpected result was found in terms of complex stability in which an interaction energy of -66.9 kcal/mol for Mono-25 is significantly more favorable those of -59.3 kcal/mol and -49.7 kcal/mol for the Di-pro and Mono-25', respectively, i.e., Mono-25 < Di-pro < Mono-25'. This trend is in contrast to an order of number of hydrogen bonds between saquinavir and HIV-1 PR in which Di-pro >> Mono-25' > Mono-25. The interaction data suggest to us to conclude that the protonated state of the active site in HIV-1 PR complexed with saquinavir inhibitor is a monoprotonated state on Asp25. In addition, the solvent effect was taken into consideration in terms of radial distribution functions and corresponding integration numbers. It was found that the HIV-1 PR pocket contains 17, 15, and 15 water molecules, coordinated in the first hydration of saquinavir.

ACKNOWLEDGMENT

Financial support by the Thailand Research Fund, grant number RTA4680008 and the generous supply of computer time by the Austrian-Thai Center for Computer-Assisted Chemical Education and Research (Bangkok, Thailand) are gratefully acknowledged. The authors wish to thank Dr. Somsak Tonmunpuean his for consultation with the research.

REFERENCES AND NOTES

- Krausslich, H.; Wimmer, E. Viral proteinases. *Annu. Rev. Biochem.* **1988**, *57*, 701–754.
- Johnston, M. I.; Hoth, D. E. Present status and future prospects for HIV Therapies. *Science* **1993**, *260*, 1286–1293.
- Levy, Y.; Caflish, A. Flexibility of Monomeric and Dimeric HIV-1 protease. *J. Phys. Chem.* **2003**, *107*, 3068–3079.
- Chen, X.; Tropsha, A. Relative binding free energies of peptide inhibitors of HIV-1 protease: the influence of the active site protonation state. *J. Med. Chem.* **1995**, *38*, 42–48.
- Ferguson, D. M.; Radmer, R. J.; Kollman, P. A. Determination of the relative binding free energies of peptide inhibitors to the HIV-1 protease. *J. Med. Chem.* **1991**, *34*, 2654–2659.
- Smith, R.; Brereton, I. M.; Chai, R. Y.; Parrinello, M. Ionization states of the catalytic residues in HIV-1 protease. *Nat. Struct. Biol.* **1996**, *3*, 946–950.
- Harte, W. E.; Beveridge, D. L. Probing structure–function relationships in human immunodeficiency virus type 1 protease via molecular dynamics simulation. *Methods Enzymol.* **1994**, *241*, 178–195.
- Wlodawer, A.; Vondrasek, J. R. INHIBITORS OF HIV-1 PROTEASE: A Major Success of Structure-Assisted Drug Design. *Annu. Rev. Biophys. Biomol. Struct.* **1998**, *27*, 249–284.
- Nam, K. Y.; Chang, H. C.; Han, C. K.; Ahn, S. K.; No, K. T. Investigation of the Protonated State of HIV-1 Protease Active Site. *Bull. Korean Chem. Soc.* **2003**, *24*, 817–823.
- Piana, S.; Sebastiani, D.; Carloni, P.; Parrinello, M. Ab Initio Molecular Dynamics-Based Assignment of the Protonation State of Pepstatin A/HIV-1 Protease Cleavage Site. *J. Am. Chem. Soc.* **2001**, *123*, 8730–8737.
- Geller, M.; Miller, M.; Swanson, S. M.; Maisel, J.; Analysis of the structure of HIV-1 protease complexed with a hexapeptide inhibitor, part II: molecular dynamic studies of the active site region. *Proteins* **1997**, *27*, 195–203.
- Hong, L.; Zhang, X. C.; Hartsuck, J. A.; Tang, J. Crystal structure of an in vivo HIV-1 protease mutant in complex with saquinavir: Insights into the mechanisms of drug resistance. *Protein Sci.* **2000**, *9*, 1898–1904.
- Case, D. A.; Pearlman, J. W.; Caldwell, T. E.; Cheatham, J., III.; Wang, W. S.; Ross, C. L.; Simmerling, T. A.; Darden, K. M.; Merz, R. V.; Stanton, A. L.; Cheng, J. J.; Vincent, M.; Crowley, V.; Tsui, H.; Gohlke, R. J.; Radmer, Y.; Duan, J.; Pitera, J.; Massova, G. L.; Seibel, U. C.; Singh, P. K.; Kollman, P. A. **2002**, AMBER 7, University of California, San Francisco.
- Bayly, C. I.; Cieplak, P.; Cornell, W. D.; Kollman, P. A. A Well-Behaved Electrostatic Potential Based Method Using Charge Restraints For Determining Atom-Centered Charges. *J. Phys. Chem.* **1993**, *97*, 10269–10280.
- Frisch, M. J.; Trucks, G. W.; Schlegel, H. B.; Scuseria, G. E.; Robb, M. A.; Cheeseman, J. R.; Zakrzewski, V. G.; Montgomery, J. A.; Stratmann, R. E. Jr.; Burant, J. C.; Dapprich, S.; Millam, J. M.; Daniels, A. D.; Kudin, K. N.; Strain, M. C.; Farkas, O.; Tomasi, J.; Barone, V.; Cossi, M.; Cammi, R.; Mennucci, B.; Pomelli, C.; Adamo, C.; Clifford, S.; Ochterski, J.; Petersson, G. A.; Ayala, P. Y.; Cui, Q.; Morokuma, K.; Malick, D. K.; Rabuck, A. D.; Raghavachari, K.; Foresman, J. B.; Cioslowski, J.; Ortiz, J. V.; Baboul, A. G.; Stefanov, B. B.; Liu, G.; Liashenko, A.; Piskorz, P.; Komaromi, I.; Gomperts, R.; Martin, R. L.; Fox, D. J.; Keith, T.; Al-Laham, M. A.; Peng, C. Y.; Nanayakkara, N.; Challacombe, M.; Gill, P. M. W.; Johnson, B.; Chen, W.; Wong, M. W.; Andres, J. L.; Gonzalez, C.; Head-Gordon, M.; Replogle, E. S.; Pople, J. A. GAUSSIAN98. (Version A.11) Gaussian, Inc., Pittsburgh, PA, 1998.
- Cornell, W. D.; Cieplak, P.; Bayly, C. I.; Gould, I. R.; Merz, K. M.; Ferguson, D. M.; Spellmeyer, D. C.; Fox, T.; Caldwell, J. W.; Kollman, P. A. A Second Generation Force Field for the Simulation of Proteins, Nucleic Acids and Organic Molecules. *J. Am. Chem. Soc.* **1995**, *117*, 5179–5197.
- Berendsen, H. J. C.; Postma, J. P. M.; van Gunsteren, W. F.; DiNola, A.; Haak, J. R.; Molecular Dynamics with coupling to an external bath. *J. Chem. Phys.* **1984**, *81*, 3684–3690.
- Rick, S. W.; Erickson, J. W.; Burt, S. K.; Reaction path and free energy calculations of the transition between alternate conformations of HIV-1 protease. *Proteins Struct. Funct. Genet.* **1998**, *32*, 7–16.
- Scott, W. R.; Schiffer, C. A. Curling of flap tips in HIV-1 protease as a mechanism for substrate entry and tolerance of drug resistance. *Structure* **2000**, *8*, 1259–1265.
- Ishima, R.; Freedberg, D. I.; Wang, Y.-X.; Louis, J. M.; Torchia, D. A. Flap opening and dimer-interface flexibility in the free and inhibitor-bound HIV protease, and their implications for function. *Structure* **1999**, *7*, 1047–1055.
- Freedberg, D. I.; Ishima, R.; Jacob, J.; Wang, Y.-X.; Kustanovich, I.; Louis, J. M.; Torchia, D. A. Rapid structural fluctuations of the free HIV protease flaps in solution: Relationship to crystal structures and comparison with predictions of dynamics calculations. *Protein Sci.* **2002**, *11*, 221–232.
- Weber, J.; Mesters, J. R.; Lepsik, M.; Prejdova, J.; Svec, M.; Sponarova, J.; Mlcochova, P.; Skalicka, K.; Strisovsky, K.; Uhlíkova, T.; Soucek, M.; Machala, L.; Stankova, M.; Vondrasek, J.; Klimkait, T.; Krausslich, H. G.; Hilgenfeld, R.; Konvalinka, J. Unusual Binding Mode of an HIV-1 protease Inhibitor Explains its Potency against Multi-drug-resistant Virus Strains. *J. Mol. Biol.* **2002**, *324*, 739–754.

- (23) Zhu, Z.; Schuster, D. I.; Tuckerman, M. E. Molecular Dynamics Study of the Connection between Flap Closing and Binding of Fullerene-Based Inhibitors of the HIV-1 Protease. *Biochemistry* **2003**, *42*, 1326–1333.
- (24) Wiley, J.; Chichester. Simulation Proton-Transfer Processes: Quantum Dynamics Embedded in a Classical Environment. Theoretical Treatment of Hydrogen Bonding. **1997**.
- (25) Wittayanarakul, K.; Aruksakunwong, O.; Chantratita, W.; Parasuk, V.; Sompornpisut, P.; Hannongbua, S. Insights into saquinavir resistance in the G48V HIV-1 protease: quantum calculations and molecular dynamic simulations. *Biophys.* **2005**, *88*, 867–879.
- (26) Wang, L.; Duan, Y.; Stouten, P.; De Lucca, G. V.; Klabe, R. M.; Kollman, P. A. Does a diol cyclic urea inhibitor of HIV-1 protease bind tighter than its corresponding alcohol form? A study by free energy perturbation and continuum electrostatics calculations. *J. Comput.-Aided. Mol. Des.* **2001**, *15*, 145–156.
- (27) Okimoto, N.; Kitayama, K.; Hata, M.; Hoshino, T.; Tsuda, M. Molecular dynamics simulations of a complex of HIV-1 protease and substrate: substrate-dependent efficiency of catalytic activity. *J. Mol. Struct. Theochem.* **2001**, *543*, 53–63.
- (28) Eurenus, K. P.; Chatfield, D. C.; Brooks, B. R. Enzyme Mechanisms with Hybrid Quantum and Molecular Mechanical Potentials. I. Theoretical Considerations. *Int. J. Quantum Chem.* **1996**, *60*, 1189–1200.

CI049784G